SPECTRAL ITERATIVE TECHNIQUES FOR THE FULL-WAVE 3D ANALYSIS OF (M)MIC STRUCTURES

Werner Wertgen* and Rolf H. Jansen**

* University of Duisburg, FB9, D-4100 Duisburg 1, WEST GERMANY
** Plessey Research Caswell Ltd., GaAs MMIC Dept., GREAT BRITAIN

ABSTRACT

As an alternative to conventional moment methods, spectral iterative techniques (SITs) are introduced for the full-wave 3d analysis of (M)MIC structures. A spectral domain integral operator formulation is used in analogy to standard scattering problems. The employed iterative computational techniques avoid the handling of large matrix equations otherwise required in the treatment of complex geometries. Hence, computation time is reduced considerably and the capability of analyzing irregular microstrip structures is obtained for problems exceeding the scope of moment methods.

INTRODUCTION

The solution of many design problems still existing today for MICs and MMICs depends to a high degree on the availability of hybrid-mode full-wave analysis tools for the characterization of microstrip type components. In particular, the analysis of (M)MIC structures "en bloc", i.e. without segmentation into substructures, is a desired goal since this allows to take into account general coupling phenomena and package effects /1/. In this respect, the contribution presented here is aimed towards the analysis of components of higher geometrical complexity avoiding increasingly larger matrices as they come along with conventional moment method solutions. The approach used here formulates a source-type integral equation in analogy to scattering problems /2/,/1/ and adapts the SIT to the full-wave, shielded 3d (M)MIC problem. Hithero, SITs have only been applied to MIC problems in the quasi-static or quasi-TEM formulation, i.e. under the assumption of zero curl of the electric field /3/-/5/.
The main advantage offered by the described SITs is that the number of mathematical operations required in the algorithms increases about linearly with M, the number of unknowns. Therefore, these techniques offer the perspective of improved computational efficiency for the analysis of complicated (M)MIC shapes. In a resently published modular approach /1/ we use Galerkin's method for analyses with up to about M = 600 expansion functions (unknowns) and with computation times growing as $M^2 \ldots M^3$. Our research on SIT appproaches presented here is a contribution made to overcome such practical limits on workstation computers.

SCATTERING FORMULATION FOR (M)MIC ANALYSIS BY ITERATIVE TECHNIQUES

For the rigorous electromagnetic 3d analysis of planar microstrip structures using SITs, a three layer lossless shielded (M)MIC-medium as shown in Fig. 1 is considered. Setting up scalar LSE and LSM electromagnetic potentials at each layer, the well known analytical spectral domain procedure /2/ leads to a linear integral equation. We introduce the operator description

$$\underline{\underline{L}}_\Omega := \iint_\Omega \underline{\underline{K}}(x,y,x',y')\, dx'\, dy' \,, \qquad x,y \in D_{tot} \quad (1)$$

where the kernel $\underline{\underline{K}}$ represents the Green's dyadic finite Fourier expansion associated with the boundary value problem. $\underline{\underline{L}}_\Omega$ is a first kind Fredholm type integral operator and maps the surface current density on a subdomain $\Omega \subset D_{tot}$ into the electric field in the x,y plane, the total (M)MIC surface area $D_{tot} = (0,a) \times (0,b)$.
In order to apply iterative computational techniques to planar circuit analysis, a specific scattering problem is formulated in analogy to standard scattering expressions in antenna or radar theory. In this context an "incident" electric field $\underline{E}_i$ is generated in the "scattering plane" (the (M)MIC substrate surface D_{tot}) using one or more impressed source current distributions $\underline{J}_{imp}$.

$$\underline{E}_i = - \underline{\underline{L}}_Q \underline{J}_{imp} \,, \qquad x,y \in D_{tot} \quad (2)$$

Here, $Q \subset D_{tot}$ is the subregion on which the impressed current density has been defined (see Fig. 1). The specific scattering problem is then formulated as

$$\underline{\underline{L}}_D \underline{J} = \underline{E}_i \,, \qquad x,y \in D. \quad (3)$$

The region D is the microstrip conductor pattern (scatterer) of the (M)MIC configuration of interest (Fig. 1).
To get the desired solution for (M)MIC characterization the source current distribution $\underline{J}_{imp}$ and the associated region Q in equation (2) must be chosen in a physically meaningful way related to the excitation of components in planar circuits. Accordingly, the source current densities $\underline{J}_{imp}$ applied are derived from those of the fundamental strip modes in the component reference planes.

0149-645X/88/0000-0709$01.00 © 1988 IEEE

It may be noted, that the operator equation (3) has only the trivial solution $\underline{J} = -\underline{J}_{imp}$ if $Q \subset D$ is choosen. Hence, the condition $Q \not\subset D$ is required, but an overlap region $Q \cap D \neq \emptyset$ may exist and is employed in our source concept (see Fig. 1 and Fig. 3). Further, the uniqueness of the solution of (3) is guaranteed except at eigenfrequencies, for which the homogeneous equation $\underline{\underline{L}}_D \cdot \underline{J} = 0$ has non-trivial solutions.

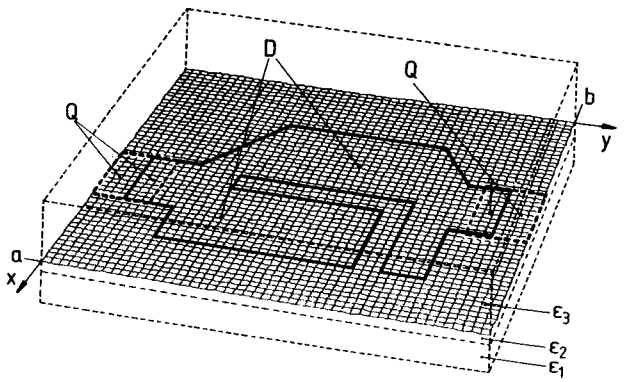

Fig. 1 General (M)MIC structure excited by impressed sources (region Q) with illustration of the discretization scheme (mesh nodes). D is the scattering domain, on which the boundary conditions have to be satisfied.

ITERATIVE TECHNIQUES AND NUMERICAL REALIZATION

Equation (3) is suited for application of the SIT in a manner as known from true scattering problems. To solve the operator equation (3) we consider two known iterative methods which propose good convergence properties:

- Van den Berg s integral-square-error computational technique, /6/-/8/, denoted as method I in the following, and
- the (generalized bi)conjugate gradient method recently described by Sarkar /9/ denoted as method II here.

Method I minimizes the integral-square-error at each iteration step n:

$$\langle \underline{R}_n, \underline{R}_n \rangle = \| \underline{R}_n \|^2 = \| \underline{\underline{L}}_D \cdot \underline{J}_n - \underline{E}_i \|^2 \qquad (4)$$

Basis functions linearly related to the residual R_n are generated in each step according to the contrast source truncation technique /6/ and are then orthogonalized completely by a Gram-Schmidt procedure in order to minimize the least square functional (4).
Method II uses the energy norm functional:

$$F(\underline{J}_n) = \langle \underline{\underline{L}}_D (\underline{J}_e - \underline{J}_n), (\underline{J}_e - \underline{J}_n) \rangle \qquad (5)$$

Since the operator in our formulation (3) is real and symmetric if suitably normalized field quantities are employed, this is completely equivalent to the ordinary conjugate gradient method. The functional (5) is minimized in each step of the iteration /9/. $\underline{J}_e$ is the exact solution to equation (3).
The realisation of SITs with the above given algorithms requires numerical representation of the operator $\underline{\underline{L}}_D$ acting on the general vector function $\underline{f}$. To achieve this, the following steps have to be carried out:

- Discretisation of the region D and approximative representation of the vector component functions f_x, f_y,
- Fourier transform of functions into spectral domain,
- Application of the operator in its spectral form,
- Inverse Fourier transform back into spatial domain.

The dyadic operator expression can be written as

$$\underline{\underline{L}}_D \cdot \underline{f} = \begin{pmatrix} \mathfrak{F}_{cs}^{-1} & 0 \\ 0 & \mathfrak{F}_{sc}^{-1} \end{pmatrix} \cdot \left\{ \begin{pmatrix} \tilde{Z}_{11} & \tilde{Z}_{12} \\ \tilde{Z}_{12} & \tilde{Z}_{22} \end{pmatrix} \cdot \begin{pmatrix} \mathfrak{F}_{cs}(\Theta f_x) \\ \mathfrak{F}_{sc}(\Theta f_y) \end{pmatrix} \right\} , \qquad (6)$$

$$\text{with} \quad \Theta = \begin{cases} 1 , & x,y \in D \\ 0 , & x,y \notin D. \end{cases} \qquad (7)$$

$\mathfrak{F}_{cs}$ is a finite 2d Fourier cosine-sine transform and $\mathfrak{F}_{sc}$ a sine-cosine transform and $\tilde{Z}$ are the spectral terms of the hybrid mode Green's dyadic.
The simplest way to discretize a shape of interest is subdivision into a rectangular 2d mesh choosing adequate resolution Δx, Δy. Representation of any 2d function is then obtained by discrete values on the grid nodes $f_x^D(m,n)$, $f_y^D(m,n)$, e.g.

$$f_x^D(m,n) = f_x(x,y) \cdot \sum_{n=0}^{N_y/2} \sum_{m=0}^{N_x/2} \delta(x-m\Delta x)\, \delta(y-n\Delta y) \qquad (8)$$

$$\text{with} \quad \Delta x = 2a/N_x, \quad \Delta y = 2b/N_y \qquad (9)$$

Arbitrarily shaped (M)MIC structures are treated simply by scanning the contour and sampling at the mesh nodes (see Fig.1). Better approximations can be obtained by convolution of the sampling values with suitable subdomain basis functions, e.g. rectangular pulse /5/, roof top /10/,/11/, or higher order types /1/. The functions represented by 2d sequences of discrete values are then transformed into the spectral domain by real discrete combined sine and cosine transforms.

$$\mathfrak{F}_{cs}^D := \text{SCAL} \sum_{n=0}^{N_y-1} \sum_{m=0}^{N_x-1} f_x^D(m,n) \cos\left(\frac{2\pi}{N_x} mi\right) \sin\left(\frac{2\pi}{N_y} nk\right) \qquad (10)$$

$\mathfrak{F}_{sc}^D$ is defined in analogy with sine and cosine functions interchanged and for inverse transforms only the scale factor SCAL is replaced. The spectral operations by multiplication with $\tilde{Z}$ are truncated by $N_x/2$, $N_y/2$.
All 2d discrete transforms defined in equation (10) are carried out numerically by very efficient appropriately specialized FFT algorithms.

RESULTS AND ILLUSTRATIONS

In order to illustrate some details of our scattering type SIT solution process, a microstrip open stub example is considered with geometrical data taken from /10/ (Fig. 2). Only the dominant longitudinal current density component J_y is considered. The transverse current density J_x can be neglected in this example. The chosen source distribution J_{yimp} with a Maxwell term in x direction and a ramp function in y direction is shown in Fig. 3. With this excitation, an electrical field E is generated according to eq. (2) and forms the right hand side of the operator eq. (3). Using a split radix FFT with $N_x = 40$ and $N_y = 80$ the SIT solution has been performed by methods I and II. The resulting solution for f = 1.3 GHz is illustrated in Fig. 4. The total current (Fig. 4a) consists of the excited portion J_y and the source portion J_{yimp}. In Fig. 4b the associated total electric field distribution is presented. Note, that the quantities J_{ytot} and E_{ytot} obtained from the numerical solution represent a superposition of source and scattered contributions. The boundary condition $E_{ytot} = 0$ is satisfied on region D only, i.e. on the microstrip metallization.

The normalized residual error for both methods employed (as implicitly defined in eq. 4) is shown in Fig. 5. For method I the normalized error decreases monotonically and reaches a value of less than 0.01% after 20 iterations. Convergence behavior of method II is not monotonic and about 5% accuracy is obtained with 20 iterations.

Using the reaction concept the frequency dependent input impedance of the stub has been calculated and compared to other results (Fig.6). We achieved good agreement with the solution obtained by our conventional approach /1/ in which also a mode related source concept is employed. The deviation from J. C. Rautio's results /10/ is mainly caused by the completely different source model used by him, which consists of only one subsectional current element and is associated with some kind of injection effect, accordingly.

To demonstrate the capability of our SIT approaches to treat irregular microstrip structures with a higher number of unknowns, the notched stub example taken from /10/,/11/ is also analyzed here. The results shown below are obtained by method II using a radix-2 FFT with $N_x = 128$, and $N_y = 128$. In Fig. 7 we illustrate the current flow and the associated component current distributions at 2 GHz. The normalized error decreases below 10% in about 5 minutes on a Micro VAX. Note, that for the solution of this example already 1712 unknown grid values have been used which by far exceeds the number of subsections in the original work /10/,/11/.

We observed that the good convergence properties of method I are deteriorated if both current components are taken into accout, while the error behavior of method II is maintained.

Again input impedance versus frequency computed with SIT II and the reaction concept is given in Fig. 8. Comparison with the original results /10/, /11/ is made. The same deviation related to the choice of the source distribution as in the open stub example are found.

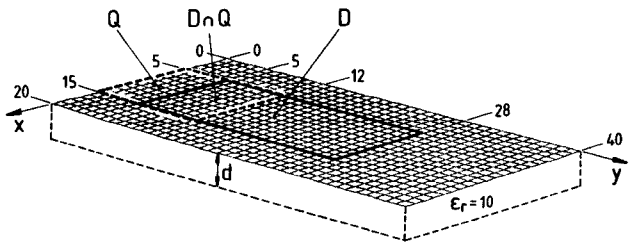

Fig. 2 Microstrip open stub with discretization and numbering of grid lines for SIT solution, geometrical data taken from /10/. Package: a = 20mm, b = 40mm, h = 50mm Substrate: d = 10mm, $\varepsilon_r = 10$

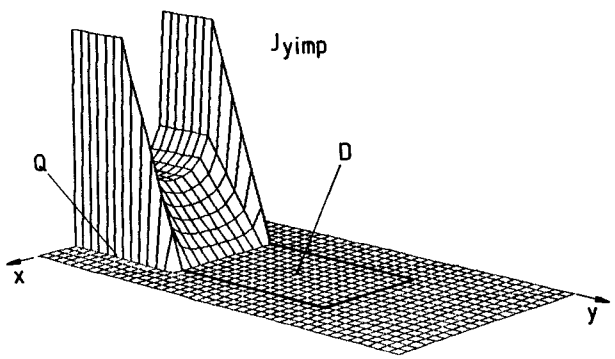

Fig. 3 Impressed source current distribution J_{yimp} at region Q.

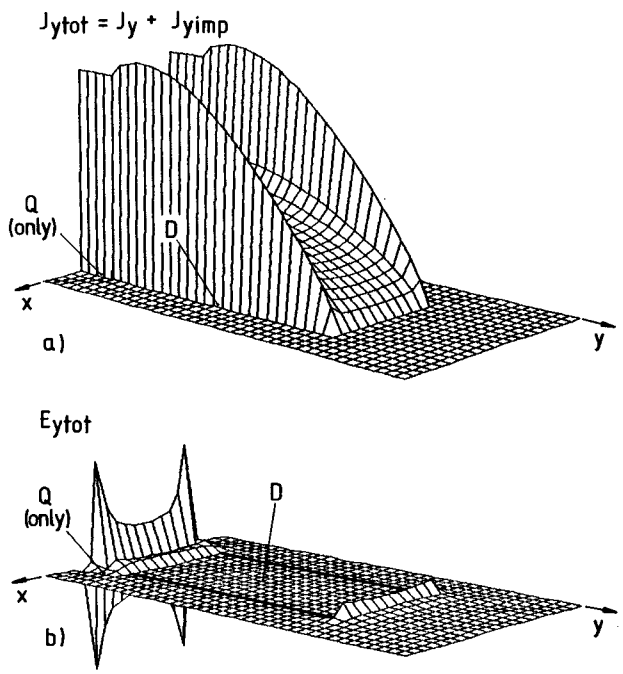

Fig. 4 Total current density J_{ytot} (a) and electric field E_{ytot} (b) in the x,y plane for SIT solution at f = 1.3 GHz.

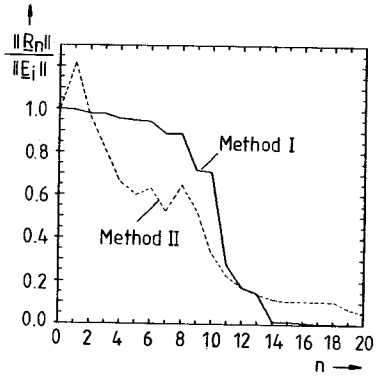

Fig. 5

Comparison of the normalized errors for both SIT methods as a function of the number of iterations (open stub example at 1.3 GHz)

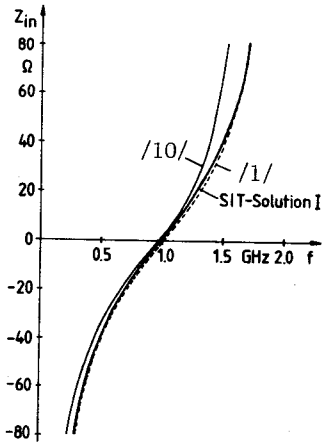

Fig. 6

Input impedance of open stub versus frequency calculated from SIT, method I. Comparison with the results of /1/ and /10/ is shown.

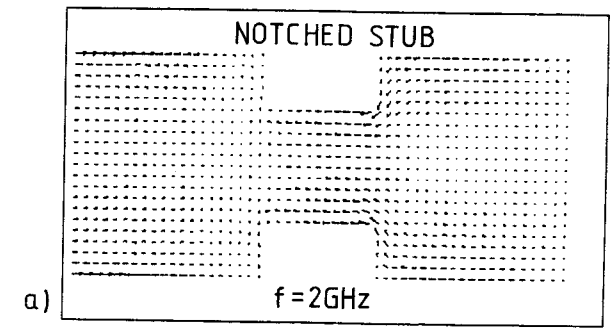

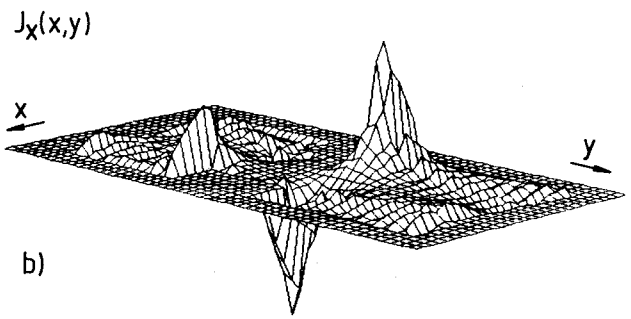

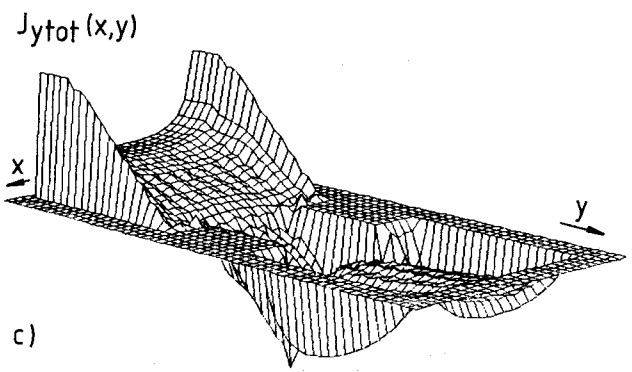

Fig. 7 Notched stub analyses example. Geometrical data taken from /11/.
a) vector surface current flow diagram at 2GHz
b) associated current component $J_x(x,y)$
c) associated total current component $J_{ytot}(x,y)$

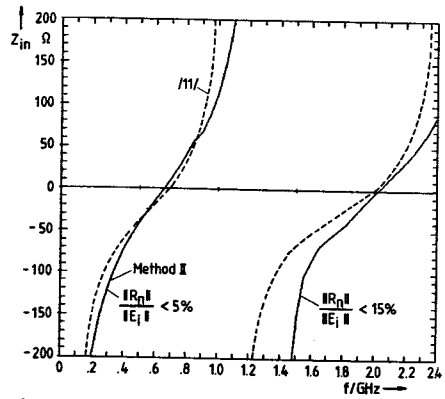

Fig. 8 Input impedance of notched stub versus frequency calculated from SIT method II. Comparison with the results of /11/ is also shown.

ACKNOWLEDGEMENTS

This work was supported by Stiftung Volkswagenwerk, West Germany, and Industr. Microwave and RF-Tech., Inc., Ratingen, West Germany

REFERENCES

/1/ Rolf H. Jansen, Werner Wertgen, 17th Europ. MW Conf. Proc., Rome 1987, 427-432
/2/ Rolf H. Jansen, MTT-33, 1985, 1043-1056.
/3/ Chi Chan, Raj Mittra, IEEE MMT-S Digest 1984, 463-465
/4/ Peter M.van den Berg, W.J. Ghijsen, A. Venema, IEEE Trans. MMT-33, 1985, 121-129
/5/ Chi Chan, Raj Mittra, IEEE Trans. MTT-36, 1988, 96-105
/6/ Peter M. van den Berg, Ant. Propag., AP-32, 1984, 1063-1072
/7/ A. J. Mackay, A. McCowen, IEEE Trans. Ant. Propag., AP-35, 1987, 218-220
/8/ Peter M. van den Berg, Walter J. Ghijsen, to be published in IEEE Trans. MTT-36, 1988
/9/ Tapan K. Sarkar, Journal of Electromagnetic Waves and Application Vol.1, 223-242, 1987
/10/ James C. Rautio, Ph.D. dissertation, Syracuse University Syracuse, NY, 1986
/11/ James C. Rautio, Roger F. Harrington, IEEE MTT-S Digest, 1987, 295-298